

Radiation effect on MHD mixed convection flow about a permeable vertical plate

Orhan Aydın · Ahmet Kaya

Received: 22 March 2008 / Accepted: 10 July 2008 / Published online: 25 July 2008
© Springer-Verlag 2008

Abstract This study investigates mixed convection heat transfer about a permeable vertical plate in the presence of magneto and thermal radiation effects. The effects of the mixed convection parameter, the radiation–conduction parameter, the surface temperature parameter, the magnetic parameter and the suction/injection parameter on the local skin friction and local heat transfer parameters are presented and analyzed.

1 Introduction

The effect of thermal radiation on convective heat transfer is very important in space technology and in processes involving high temperatures such as nuclear power plants, gas turbines and thermal energy storage.

Alam et al. [1] analyzed a two-dimensional steady MHD mixed convection and mass transfer flow over a semi-infinite porous inclined plate in the presence of thermal radiation with variable suction and thermophoresis. Yih [2] studied the effect of radiation on mixed convection flow optically dense viscous fluids about an isothermal wedge embedded in a saturated porous medium. Al-Odat et al. [3] investigated the influences of radiation on mixed convection flow of an optically dense viscous fluid along an isothermal wedge embedded in non-Darcy porous medium. Chamkha et al. [4] investigated on the steady-state, hydromagnetic forced convective boundary-layer flow of an incompressible Newtonian, electrically conducting and heat-generating/

absorbing fluid over a non-isothermal wedge in the presence of thermal radiation effects. Elbashbeshy and Bazid [5] determined the effect of radiation on forced convection flow of a micropolar fluid over a horizontal plate. Hossain and Takhar [6] analyzed the effect of radiation using the Rosse-land diffusion approximation on mixed convection along a vertical plate with uniform free stream velocity and surface temperature. Hossain et al. [7] determined the effect of radiation on the natural convection flow of an optically dense incompressible fluid along a uniformly heated vertical plate with a uniform suction. Hossain et al. [8] investigated effect of thermal radiation on the natural convection flow along a uniformly heated vertical porous plate with variable viscosity and uniform suction velocity. Duwairi [9] and Damseh et al. [10] studied the radiation and magnetic effects on the skin friction and heat transfer for forced convection conditions.

The study of magneto-hydrodynamic flow for an electrically conducting fluid past a heated surface has attracted the interest of many researchers in view of its important applications in many engineering problems such as plasma studies, petroleum industries, MHD power generators, cooling of nuclear reactors, the boundary layer control in aerodynamics, and crystal growth [10, 11]. Chen [11] investigated the momentum, heat and mass transfer characteristics of MHD natural convection flow over a permeable, inclined surface with variable wall temperature and concentration, taking into consideration the effects of ohmic heating and viscous dissipation. Seddeek [12] analyzed the effect of variable viscosity and magnetic field on the flow and heat transfer past a continuously moving porous plate. Abdelkhalek [13] investigated the effects of mass transfer on steady two-dimensional laminar MHD mixed convection. Aldoss and Ali [14] studied the effects of suction and blowing on convection heat transfer from a horizontal cylinder in cross magnetohydrodynamic flow.

O. Aydın (✉) · A. Kaya
Department of Mechanical Engineering,
Karadeniz Technical University, 61080 Trabzon, Turkey
e-mail: oaydin@ktu.edu.tr

Nanousis [15] analyzed the effects of an applied magnetic field on the mixed convection boundary-layer flow over a wedge with suction or injection.

The aim of the present study is focused at highlighting the combined effects of gas radiation and magnetic field on the mixed convection flow from a permeable vertical plate.

2 Analysis

Consider a semi-infinite vertical permeable plate at a uniform temperature T_w which is played vertical in a quiescent fluid of infinite extent at constant temperature T_∞ . The fluid is assumed to be a gray, emitting and absorbing, but non-scattering medium. The following assumptions are made in the analysis: (a) variations in fluid properties are limited only to those density variations which affect the buoyancy terms, (b) viscous dissipation effects are negligible, and (c) the radiative heat flux in the x -direction is considered negligible in comparison with that in the y -direction, where the physical coordinates (x, y) are chosen such that x is measured from the leading edge in the streamwise direction and y is measured normal to the surface of the plate. The coordinates system and the flow configuration are shown in Fig. 1.

Under the usual Boussinesq approximation, the conservation equations for the steady, laminar, two-dimensional boundary-layer flow problem under consideration can be written as

$$\frac{\partial u}{\partial x} + \frac{\partial v}{\partial y} = 0 \tag{1}$$

$$u \frac{\partial u}{\partial x} + v \frac{\partial u}{\partial y} = \nu \frac{\partial^2 u}{\partial y^2} + g \beta (T - T_\infty) - \frac{\sigma B_0^2}{\rho} (u - u_\infty) \tag{2}$$

$$u \frac{\partial T}{\partial x} + v \frac{\partial T}{\partial y} = \frac{\nu}{Pr} \left(\frac{\partial^2 T}{\partial y^2} \right) - \frac{1}{\rho c_p} \frac{\partial}{\partial y} (q_R) \tag{3}$$

Here u and v are the velocity components in the x and y -direction, respectively, T is the temperature of the fluid, β is the coefficient of thermal expansion, ν is the kinematic viscosity, ρ is the fluid density, g is the acceleration due to gravity, σ is the electrical conductivity of the fluid and B_0 is the magnetic flux density.

The quantity q_R on the right-hand side of Eq. (3) represents the radiative heat flux in the y -direction. For simplicity and comparison, the radiative heat flux term in the energy equation is analyzed by utilizing the Rosseland diffusion approximation [16] for an optically thick boundary layer as follows:

$$q_r = -\frac{4a}{3\alpha_R} \frac{\partial T^4}{\partial y} \quad \text{and} \quad \frac{\partial q_r}{\partial y} = -\frac{16a}{3\alpha_R} \frac{\partial}{\partial y} \left(T^3 \frac{\partial T}{\partial y} \right) \tag{4}$$

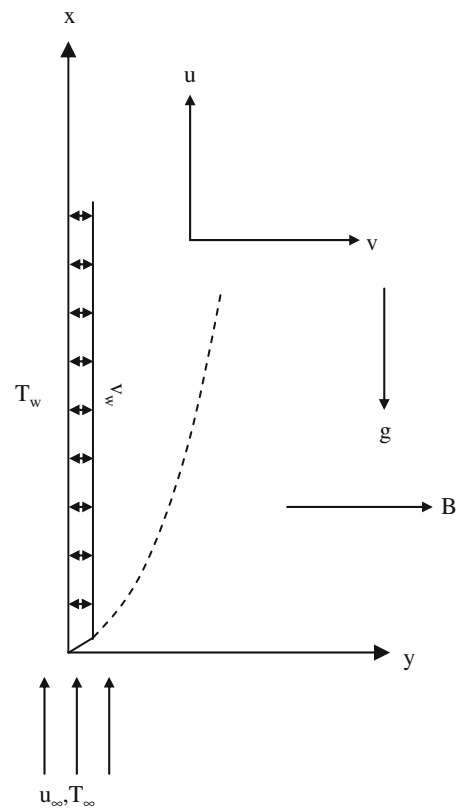


Fig. 1 The schematic of the problem

where a is the Stefan–Boltzmann constant, α_R is the Rosseland mean absorption coefficient. This approximation is valid at points optically far from the bounding surface, and is good only for intensive absorption, that is, for an optically thick boundary layer [8].

The appropriate boundary conditions for the velocity and temperature of this problem are

$$\begin{aligned} x = 0 \quad y > 0 \quad T = T_\infty \quad u = u_\infty \\ x > 0 \quad y = 0 \quad T = T_w \quad u = 0 \quad v = \pm V_w \\ y \rightarrow \infty \quad T \rightarrow T_\infty \quad u \rightarrow u_\infty \end{aligned} \tag{5}$$

The minus sign for the conductive gray fluid vertical velocity means the suction from the permeable wall, where the plus sign means the gray fluid injection. To seek a solution, the following dimensionless variables are introduced:

$$\begin{aligned} \xi = \frac{x}{L}, \quad \psi(x, y) = (\nu u_\infty x)^{1/2} f(\xi, \eta), \quad \eta = y \left(\frac{u_\infty}{\nu x} \right)^{1/2}, \\ \theta = \frac{T - T_\infty}{T_w - T_\infty} \end{aligned} \tag{6}$$

where $\psi(x, y)$ is the free stream function that satisfies Eq. (1) with $u = \partial\psi/\partial y$ and $v = -\partial\psi/\partial x$.

In terms of these new variables, the velocity components can be expressed as

$$u = u_\infty f', \tag{7}$$

$$v = -\frac{(vu_\infty x)^{1/2}}{x} \left\{ \frac{1}{2} f + \xi \frac{\partial f}{\partial \xi} - \frac{\eta}{2} f' \right\} \tag{8}$$

The transformed momentum and energy equations together with the boundary conditions, Eqs. (2), (3) and (5), can be written as

$$f''' + \frac{1}{2} f f'' + Ri \zeta \theta - M \zeta (f' - 1) = \zeta \left(f' \frac{\partial f'}{\partial \xi} - f'' \frac{\partial f}{\partial \xi} \right) \tag{9}$$

$$\begin{aligned} \frac{1}{Pr} \theta'' + \frac{1}{2} f \theta' + \frac{4}{3PrR_d} \left\{ [\theta(\theta_w - 1) + 1]^3 \theta' \right\}' \\ = \zeta \left(f' \frac{\partial \theta}{\partial \xi} - \theta' \frac{\partial f}{\partial \xi} \right) \end{aligned} \tag{10}$$

with the boundary conditions;

$$\begin{aligned} f(\zeta, 0) + 2\zeta \frac{\partial f}{\partial \zeta} = f_w \zeta^{1/2}, \quad f'(\zeta, 0) = 0, \quad \theta(\zeta, 0) = 1, \\ f'(\zeta, \infty) = 1, \quad \theta(\zeta, \infty) = 0 \end{aligned} \tag{11}$$

where $f_w = -2\frac{L}{v} V_w Re_L^{-1/2}$, the case $f_w > 0$ designates suction while $f_w < 0$ indicates injection or blowing. The corresponding dimensionless groups that appeared in the governing equations defined as

$$\begin{aligned} Pr = \frac{\mu c_p}{k} = \frac{\nu}{\alpha}, \quad Ri = \frac{Gr}{Re^2}, \quad Gr = \frac{g\beta(T_w - T_\infty)L^3}{\nu^2}, \\ Re = \frac{u_\infty L}{\nu}, \quad M = Ha/Re \\ Ha = \frac{\sigma B_0^2 L^2}{\mu}, \quad R_d = \frac{k\alpha_R}{4aT_\infty^3}, \quad \text{and} \quad \theta_w = \frac{T_w}{T_\infty} \end{aligned} \tag{12}$$

where Pr is the Prandtl number, Ri is the Richardson number, Gr is the Grashof number, Re is the Reynolds number, M is the magnetic parameter which is the ratio of the Hartman number to the Reynolds number, Ha is the Hartman number, R_d is the Planck number (radiation–conduction parameter), θ_w is the surface temperature ratio to the ambient fluid.

In the above system of equations, the radiation–conduction parameter is absent from the MHD mixed convection heat transfer problem when $R_d \rightarrow \infty$. It should be mentioned that the optically thick approximation should be valid for relatively low values of the radiation–conduction parameter, R_d . According to Ali et al. [17], some values of R_d for different gases are: (1) $R_d = 10–30$: carbon dioxide (100–650°F) with corresponding Prandtl number range 0.76–0.6; (2) $R_d = 30–200$: ammonia vapor (120–400°F) with corresponding Prandtl number range 0.88–0.84; (3) $R_d = 30–200$: water vapor (220–900°F) with corresponding Prandtl number 1.

The system of transformed equations together with the boundary conditions, Eqs. (9)–(11), have been solved

numerically using the Keller box scheme, an efficient and accurate finite-difference scheme, similar to that described in Cebeci and Bradshaw [18]. For the sake of brevity, details of the numerical method are not described, referring the reader to Cebeci and Bradshaw [18]. This is a very popular implicit scheme, which demonstrates the ability to solve systems of differential equations of any order as well as featuring second-order accuracy (which can be realized with arbitrary non-uniform spacing), allowing very rapid x or ζ (streamwise distance) variations [10]. In the calculations, a uniform grid of the step size 0.01 in the η -direction and a nonuniform grid in the ζ -direction with a starting step size 0.001 and an increase of 0.05 times the previous step size were found to be satisfactory in obtaining sufficient accuracy within a tolerance better than 10^{-6} in nearly all cases.

3 Results and discussion

At first, in order to verify the accuracy of the numerical results, the validity of the numerical code developed has been checked for some limiting cases. For $Pr = 1.0$, $Ri = 0.0$, and $R_d \rightarrow \infty$, we compare our $-\theta'(0, 0)$ results with those given by Chamkha et al. [4], Lin and Lin [19], Yih [20] and Nield and Kuznetsov [21] (Table 1). For different f_w and ζ , we compare our $-\theta'(\zeta, 0)$ results with those given by Chamkha et al. [22] (Table 2). As it is seen from Tables 1 and 2 excellent agreements have been observed.

In this paper, the mixed convection effects of ionized gas adjacent to radiate porous wall are investigated including the magnetic field. The following ranges of the main parameters are considered: $Ri = 0, 1, 2$ and 3 ; $Pr = 1.0$; $f_w = -0.1, 0.0, 0.1$; magnetic parameter $M = 1, 2$ and 3 ; radiation parameter $R_d = 1, 10$, and 50 ; and surface temperature parameter $\theta_w = 1.7, 2.0$, and 2.3 . The mixed convection parameter Ri , the radiation parameter R_d , the surface temperature parameter θ_w , the suction/injection effects f_w and magnetic parameter M on the momentum and

Table 1 Comparison of the values $-\theta'(0, 0)$ for various values Pr at $Ri = 0.0, M = 0.0, R_d \rightarrow \infty$ and $f_w = 0.0$

| Pr | Chamkha et al. [4] | Lin and Lin [19] | Yih [20] | Nield and Kuznetsov [21] | Present study |
|------|--------------------|------------------|----------|--------------------------|---------------|
| 0.01 | 0.051830 | 0.051559 | 0.051589 | – | 0.051437 |
| 0.1 | 0.142003 | 0.140032 | 0.140034 | 0.1580 | 0.148123 |
| 1 | 0.332173 | 0.332057 | 0.332057 | 0.3320 | 0.332000 |
| 10 | 0.728310 | 0.728148 | 0.728141 | 0.7300 | 0.727801 |
| 100 | 1.572180 | 1.571860 | 1.571831 | 1.5700 | 1.573141 |

Table 2 Comparison of the values $-\theta'(\xi, 0)$ for various values ξ and f_w at $M = 1$, $Ri = 1$, $R_d \rightarrow \infty$ and $Pr = 0.7$

| ξ | $f_w = 1.0$ | | $f_w = 0.0$ | | $f_w = -1.0$ | |
|-------|---------------------|---------------|---------------------|---------------|---------------------|---------------|
| | Chamkha et al. [22] | Present study | Chamkha et al. [22] | Present study | Chamkha et al. [22] | Present study |
| 0.0 | 0.2930 | 0.2926 | 0.2930 | 0.2926 | 0.2930 | 0.2926 |
| 0.1 | 0.4550 | 0.4509 | 0.3220 | 0.3297 | 0.2100 | 0.2166 |
| 0.2 | 0.5420 | 0.5428 | 0.3250 | 0.3497 | 0.2000 | 0.2013 |
| 0.3 | 0.6000 | 0.5954 | 0.3630 | 0.3665 | 0.1910 | 0.1924 |
| 0.4 | 0.6600 | 0.6599 | 0.3800 | 0.3793 | 0.1900 | 0.1876 |
| 0.5 | 0.7000 | 0.6935 | 0.3900 | 0.3904 | 0.1780 | 0.1809 |
| 0.6 | 0.7400 | 0.7346 | 0.4000 | 0.3997 | 0.1690 | 0.1772 |
| 0.7 | 0.7800 | 0.7834 | 0.4090 | 0.4080 | 0.1700 | 0.1717 |
| 0.8 | 0.8180 | 0.8173 | 0.4100 | 0.4153 | 0.1630 | 0.1683 |

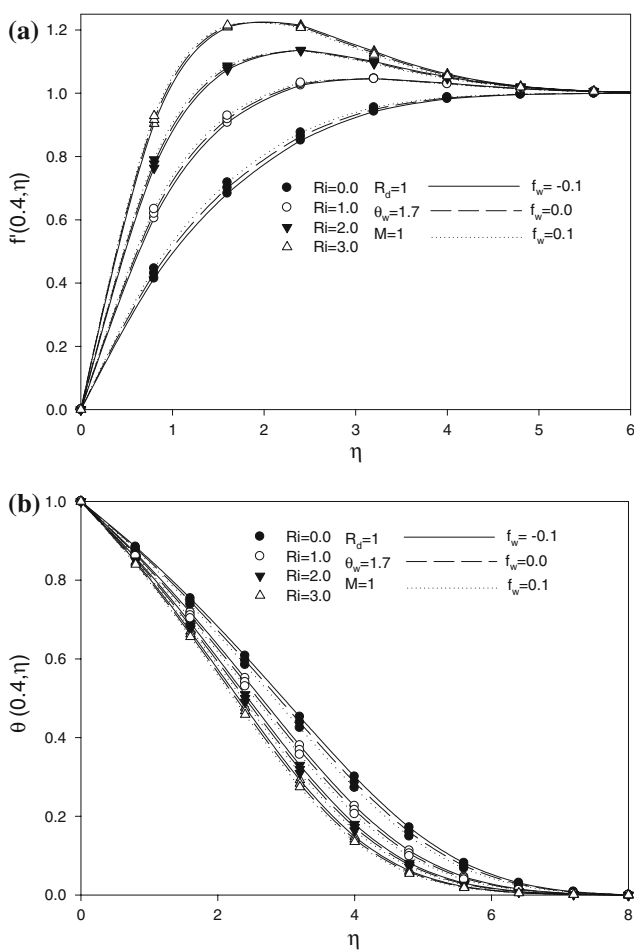


Fig. 2 Dimensionless velocity (a) and temperature (b) profiles for different Ri while $Pr = 1.0$, $M = 1$, $R_d = 1$, $\theta_w = 1.7$ and $\zeta = 0.4$

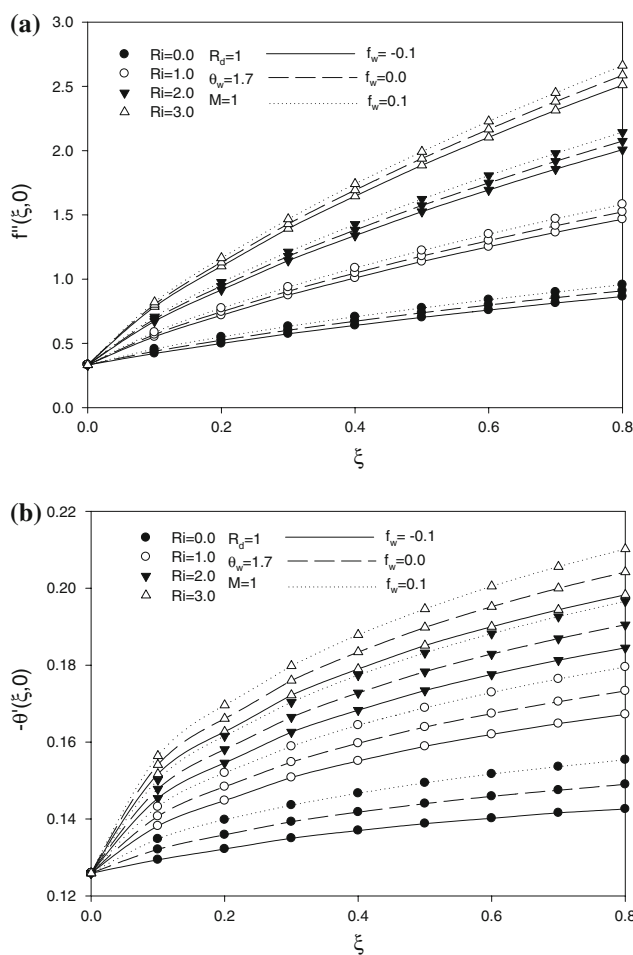


Fig. 3 Numerical values of local skin friction (a) and local heat transfer (b) against the streamwise distance ζ for different Ri while $Pr = 1.0$, $M = 1$, $R_d = 1$ and $\theta_w = 1.7$

heat transfer are analyzed and discussed. The Richardson number, Ri represents a measure of the effect of the buoyancy in comparison with that of the inertia of the external forced or free stream flow on the heat and fluid flow. Outside the mixed convection region, either the pure

forced convection or the free convection analysis can be used to describe accurately the flow or the temperature field. Forced convection is the dominant mode of transport when $Ri \rightarrow 0$, whereas free convection is the dominant

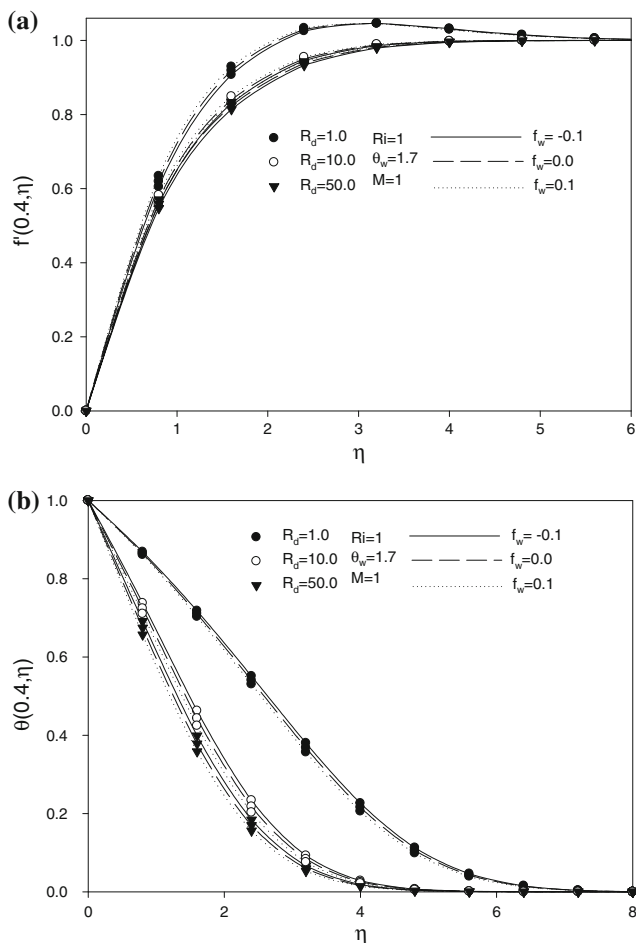


Fig. 4 Dimensionless velocity (a) and temperature (b) profiles for different R_d while $Pr = 1.0$, $M = 1$, $Ri = 1$, $\theta_w = 1.7$ and $\zeta = 0.4$

mode when $Ri \rightarrow \infty$. Buoyancy forces can enhance the surface heat transfer rate when they assist the forced convection, and vice versa [23].

Figure 2 shows the effect of the buoyancy parameter Ri on the dimensionless velocity and temperature profiles. The velocity and temperature gradients increase with Ri and the momentum and thermal boundary layers decrease.

The effect of injection/suction of fluid from the plate on the dimensionless velocity and temperature profiles is also clear from Fig. 2. Injecting fluid into the boundary layer broadens the velocity distribution and increases the hydrodynamic boundary layer thicknesses. Also, the wall shear stress would be increased with the application of suction whereas injection tends to decrease wall shear stress. This can be explained by the fact that the wall velocity gradient is increased with the increasing value of f_w . The effect of injection is found to broaden the temperature distribution, decrease the wall temperature gradient, and hence reduce the heat transfer rate. On the

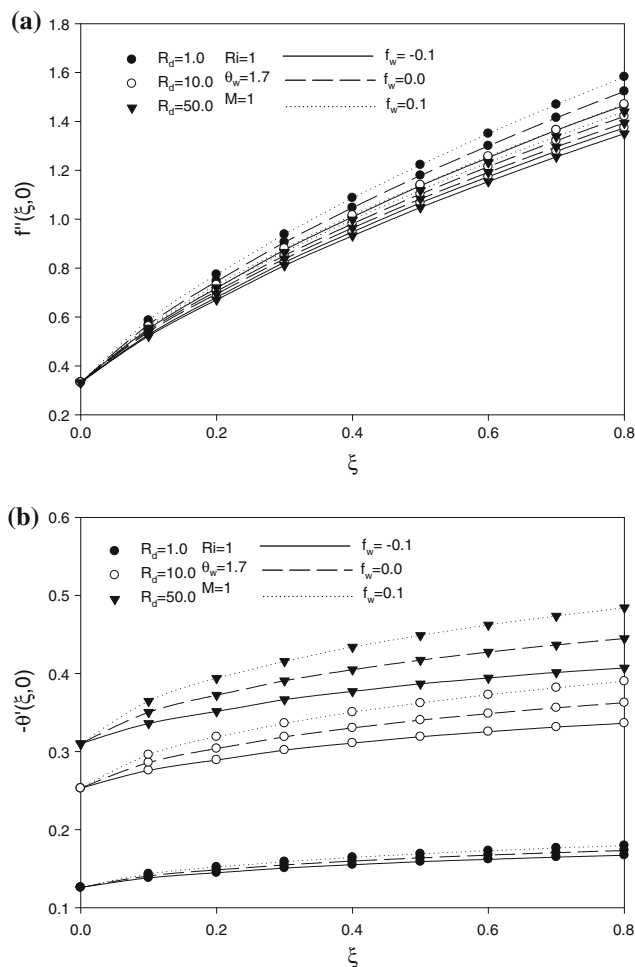


Fig. 5 Numerical values of local skin friction (a) and local heat transfer (b) against the streamwise distance ζ for different R_d while $Pr = 1.0$, $M = 1$, $Ri = 1$ and $\theta_w = 1.7$

other hand, the thermal boundary layer becomes thinner and the wall temperature gradient becomes larger when suction is applied.

The effect of the mixed convection parameter Ri on the local skin friction and the local heat transfer parameters are shown in Fig. 3. Both the local skin friction and the local heat transfer parameters increase with an increase in the mixed convection parameter Ri .

Figure 4 shows the dimensionless velocity and temperature profiles inside the boundary layer for different values of the radiation parameter R_d . The increasing of the radiation parameter R_d increases the momentum boundary layer thickness and decreases the temperature boundary layer thickness (i.e. increases temperature gradients at the permeable wall).

In Fig. 5 the effects of the radiation parameter R_d on the local skin friction and the local heat transfer parameters are displayed. The increasing of the radiation parameter R_d

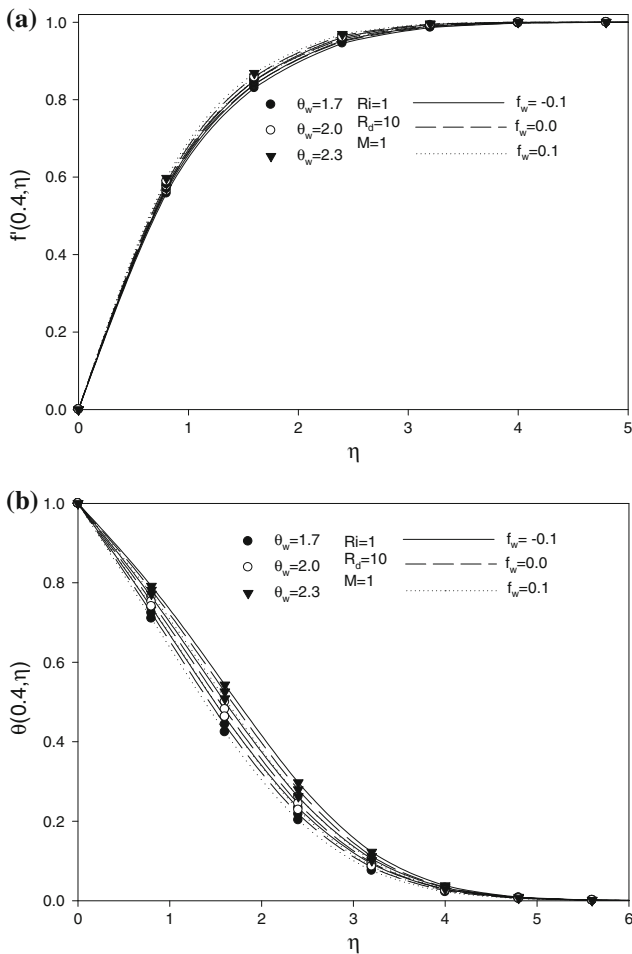


Fig. 6 Dimensionless velocity (a) and temperature (b) profiles for different θ_w while $Pr = 1.0$, $M = 1$, $Ri = 1$, $R_d = 1$ and $\zeta = 0.4$

decreases the local skin friction parameter and increases the local heat transfer parameter as a result of increased hydrodynamic boundary layer thickness and decreased thermal boundary layer thickness.

The effect of surface temperature parameter θ_w on the velocity and temperature profiles is shown in Fig. 6. Increasing the surface temperature ratio increases dimensionless velocity profile (Fig. 6), which is shown to increase the local skin friction parameter (Fig. 7). Moreover increasing the temperature ratio also increased the temperatures inside the boundary layer (Fig. 6) and consequently decreases the local heat transfer parameter (Fig. 7).

Figure 8 shows the dimensionless velocity and temperature profiles inside the boundary layer for different values of the magnetic parameter M . The increasing of the magnetic parameter M decreases the momentum and the temperature boundary layer thicknesses (i.e. increases velocity and temperature gradients at the permeable wall).

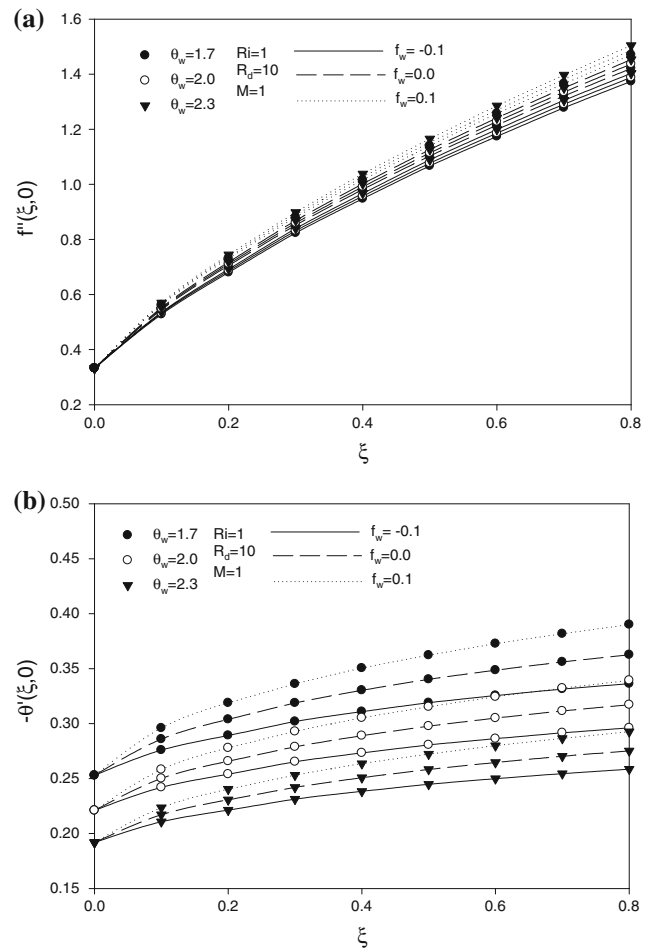


Fig. 7 Numerical values of local skin friction (a) and local heat transfer (b) against the streamwise distance ζ for different θ_w while $Pr = 1.0$, $M = 1$, $Ri = 1$ and $R_d = 1$

Both the local skin friction and the local heat transfer parameters increase with the magnetic parameter M (Fig. 9). Since the magnetic parameter M is multiplied by ζ [see Eq. (9)], the effect of M increases with the streamwise distance ζ .

It is also clear from Figs. 3, 5, 7, and 9 increasing f_w increases local skin friction and local heat transfer parameter.

4 Conclusions

In this article, we have studied numerically the effects of suction/injection and thermal radiation on a steady MHD mixed convective flows of a viscous incompressible fluid about a permeable vertical plate. A transformed set of non-similar equations have been solved using the Keller box scheme, an efficient and accurate finite-difference scheme.

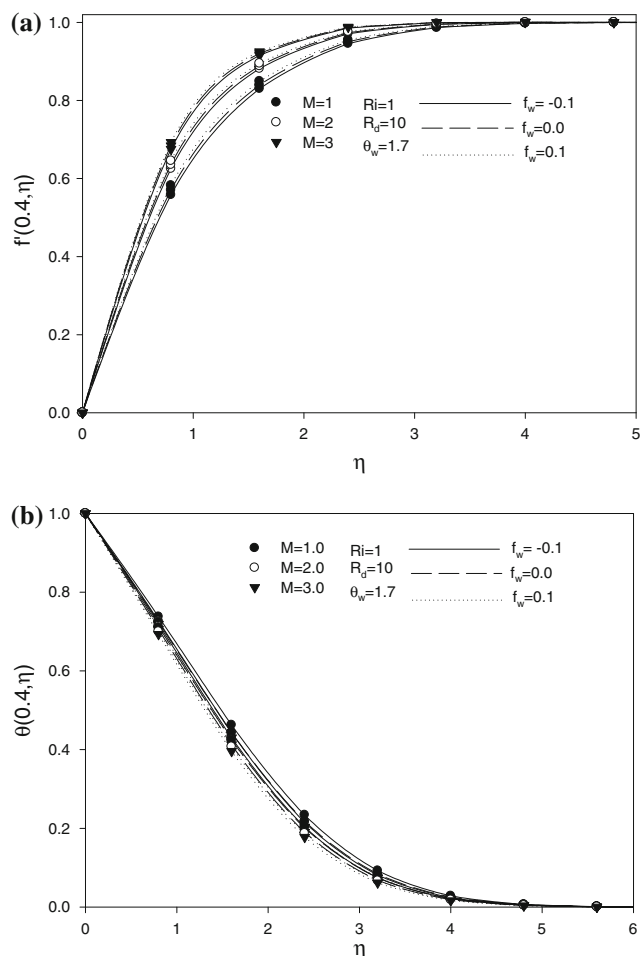


Fig. 8 Dimensionless velocity (a) and temperature (b) profiles for different M while $Pr = 1.0$, $Ri = 1$, $R_d = 1$, $\theta_w = 1.7$ and $\xi = 0.4$

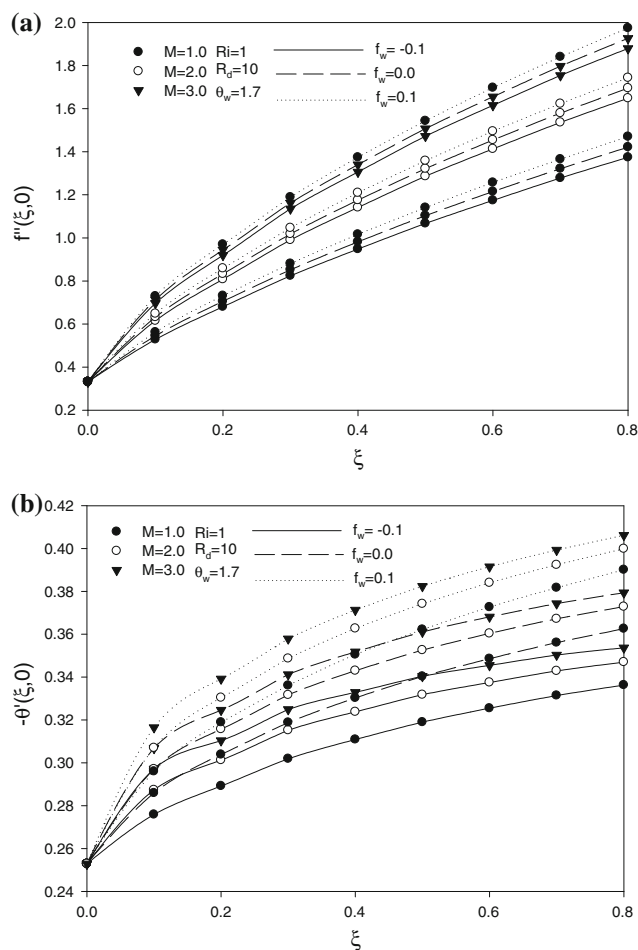


Fig. 9 Numerical values of local skin friction (a) and local heat transfer (b) against the streamwise distance ξ for different M while $Pr = 1.0$, $Ri = 1$, $R_d = 1$ and $\theta_w = 1.7$

From the present numerical investigation, the following conclusions can be drawn:

1. An increase in the mixed convection parameter increases the local skin friction and the local heat transfer parameters.
2. An increase in the radiation parameter decreases the local skin friction parameter and increases the local heat transfer parameter.
3. An increase in the surface temperature parameter increases the local skin friction parameter and decreases the local heat transfer parameter.
4. An increase in the magnetic parameter increases the local skin friction and the local heat transfer parameters.
5. It is found that the presence of suction makes the thermal boundary layer thinner and therefore enhances the heat transfer, while the injection presents an opposite effect.

References

1. Alam MS, Rahman MM, Sattar MA (2008) Effects of variable suction and thermophoresis on steady MHD combined free-forced convective heat and mass transfer flow over a semi-infinite permeable inclined plate in the presence of thermal radiation. *Int J Therm Sci* 47(6):758–765
2. Yih KA (2001) Radiation effect on mixed convection over an isothermal wedge in porous media: the entire regime. *Heat Transf Eng* 22:26–32
3. Al-Odat MQ, Al-Hussien FMS, Damseh RA (2005) Influence of radiation on mixed convection over a wedge in non-Darcy porous medium. *Forsch Ingenieur* 69:209–215
4. Chamkha AJ, Mujtaba M, Quadri A, Issa C (2003) Thermal radiation effects on MHD forced convection flow adjacent to a non-isothermal wedge in the presence of heat source or sink. *Heat Mass Transf* 39:305–312
5. Elbashbeshy EMA, Bazid MAA (2000) Effect of radiation on forced convection flow of a micropolar fluid over a horizontal plate. *Can J Phys* 78:907–913
6. Hossain MA, Takhar HS (1996) Radiation effects on mixed convection along a vertical plate with uniform surface temperature. *Heat Mass Transf* 31:243–248

7. Hossain MA, Alima MA, Rees DAS (1999) The effect of radiation on free convection from a porous vertical plate. *Int J Heat Mass Transf* 31:181–191
8. Hossain MA, Khanfer K, Vafai K (2001) The effect of radiation on free convection flow of fluid with variable viscosity from a porous vertical plate. *Int J Therm Sci* 40:115–124
9. Duwairi HM (2005) Viscous and joule heating effects on forced convection flow from radiate isothermal porous surfaces. *Int J Numer Method Heat Fluid Flow* 15:429–440
10. Damseh RA, Duwairi HM, Al-Odat M (2006) Similarity analysis of magnetic field and thermal radiation effects on forced convection flow. *Turk J Eng Env Sci* 30:83–89
11. Chen CH (2004) Heat and mass transfer in MHD flow by natural convection from a permeable, inclined surface with variable wall temperature and concentration. *Acta Mech* 172:219–235
12. Seddeek MA (2000) The effect of variable viscosity on hydro-magnetic flow and heat transfer past a continuously moving porous boundary with radiation. *Int Comm Heat Mass* 27(7):1037–1046
13. Abdelkhalek MM (2006) The skin friction in the MHD mixed convection stagnation point with mass transfer. *Int Comm Heat Mass* 33:249–258
14. Aldoss TK, Ali YD (1997) MHD free forced convection from a horizontal cylinder with suction and blowing. *Int Comm Heat Mass* 24(5):683–693
15. Nanousis ND (1999) Theoretical magnetohydrodynamic analysis of mixed convection boundary layer flow over a wedge with uniform suction or injection. *Acta Mech* 138:21–30
16. Sparrow EM, Cess RD (1961) Free convection with blowing or suction. *J Heat Transf* 83:387–396
17. Ali MM, Chen TS, Armaly BF (1984) Natural convection–radiation interaction in boundary-layer flow over horizontal surfaces. *AIAA J* 22:1797–1803
18. Cebeci T, Bradshaw P (1984) *Physical and computational aspects of convective heat transfer*. Springer, New York
19. Lin HT, Lin LK (1987) Similarity solutions for laminar forced convection heat transfer from wedges to fluids of any Prandtl number. *Int J Heat Mass Transf* 30:1111–1118
20. Yih KA (1999) MHD forced convection flow adjacent to a non-isothermal wedge. *Int Comm Heat Mass Transf* 26:819–827
21. Kuznetsov AV, Nield DA (2006) Boundary layer treatment of forced convection over a wedge with an attached porous substrate. *J Porous Media* 9(7):683–694
22. Chamkha AJ, Takhar HS, Nath G (2004) Mixed convection flow over a vertical plate with localized heating (cooling), magnetic field and suction (injection). *Heat Mass Transf* 40:835–841
23. Aydin O, Kaya A (2007) Mixed convection of a viscous dissipating fluid about a vertical flat plate. *Appl Math Model* 31:843–853